Experimental Determination of Billiard Wave Functions

J. Stein and H.-J. Stöckmann
Fachbereich Physik, Universität Marburg, D-W-3550 Marburg, Federal Republic of Germany
(Received 11 October 1991)

Wave functions of a stadium billiard are determined in a microwave analog experiment. It is shown that Gutzwiller's semiclassical representation of the Green's function in terms of classical trajectories can account not only for eigenvalue spectra but also for eigenfunction patterns.

PACS numbers: 05.45.+b

The perhaps most impressive way to demonstrate the qualitative difference between integrable and nonintegrable systems is the presentation of eigenfunction patterns of billiards. Whereas for a rectangular or circular billiard the nodal lines form a regular grid with a large number of crossings, for nonintegrable billiards the node lines perform meandric walks while avoiding any crossing (in the presence of degeneracies the crossings can be destroyed by suitable superpositions of eigenfunctions also in integrable billiards; for details see Chap. 15 of Ref. [1]). This was first demonstrated by McDonald and Kaufman [2] who calculated wave functions in a stadium billiard (a more detailed account of this work can be found in Ref. [3]). A surprise was then the discovery by Heller that many wave functions are not distributed more or less uniformly over the whole billiard but form so-called scars, regions of extra high amplitudes near classical periodic orbits [4,5]. An approach to explain these scars was made by Bogomolny [6]. He used the fact that the Green's function,

$$G(q_A,q_B,E)=\sum_n \frac{\varphi_n^*(q_A)\varphi_n(q_B)}{E-E_n}\,, \tag{1}$$

can be expressed semiclassically as a sum over classically allowed trajectories [7],

$$G(q_A,q_B,E)\approx \frac{1}{i(2\pi i)^{1/2}}\sum_r |\Delta_r|^{1/2}\exp\left(\frac{i}{\hbar}S_r(q_A,q_B,E)-im_r\frac{\pi}{2}\right). \tag{2}$$

In Eq. (1) E_n and $\varphi_n(q)$ denote eigenenergy and eigenfunction of the nth eigenvalue, respectively. In Eq. (2) the sum is over all trajectories starting at q_A and ending at q_B. $S_r(q_A,q_B,E)$ is the classical action for the trajectory, and m_r is the Maslov index counting the number of conjugated points. For billiards the action is given by $S(q_A,q_B,E)=\hbar kq$. Here q denotes the total length of the trajectory and $k=\sqrt{2mE}/\hbar$ is the de Broglie wave number of the particle. The Maslov index is given by $m_r=2n_r$, where n_r is the number of reflections (for a billiard with hard walls every reflection gives rise to a phase jump of π). The prefactor $|\Delta_r|^{1/2}$ entering into Eq. (2) takes into account the stability of the trajectory. Δ_r can be written as a Jacobian determinant,

$$\Delta_r=|\partial p_A^\alpha(q_A,q_B,E)/\partial q_B^\beta|,\quad \alpha,\beta=1,2\,, \tag{3}$$

where the p_A^α are the two components of the momentum at the starting point, written as functions of q_A,q_B,E, and q_B^β are the two components of the end position. Classically, Δ_r is proportional to the density of trajectories at point q_B starting isotropically from point q_A (a very readable account of these questions can be found in Ref. [8]).

Taking $q_A=q_B=q$ in Eq. (2) and integrating over q, one gets the Gutzwiller trace formula establishing a correspondence between periodic orbits and the quantum-mechanical spectrum. This correspondence could be demonstrated experimentally by the present authors for electromagnetic eigenfrequency spectra of billiard-shaped microwave resonators (Ref. [9], hereafter denoted by I).

In I the equivalence of the two-dimensional time-independent Schrödinger equation and the time-independent wave equation was used for an experimental determination of the quantum-mechanical eigenvalues. The question arose whether a similar determination of eigenfunctions was also possible. In fact, a first famous analog experiment of this type was performed already 200 years ago by E. F. Chladni who studied nodal patterns of vibrating plates. Even Chladni figures for irregular shapes were already observed in the last century but could not be interpreted at that time [10]. Figure 1 shows a modern Chladni figure on a glass plate with the shape of a quartered Sinai billiard. The meandric shape of nodal lines first observed by McDonald and Kaufman in their calculations on a stadium billiard can be observed already with this extremely simple device. Comparably simple is the experimental realization of wave chaos on water surfaces [11].

Both mentioned arrangements are very well suited for demonstration purposes but probably not for quantitative measurements. Here again billiard-shaped microwave resonators offer an alternative. It was shown in I that the microwave reflection from such resonators measured as a function of frequency shows minima whenever the irradiated frequency corresponds to an eigenfrequency of the resonator. The reflected microwave power is proportional to the energy density at the coupling wire, i.e., to the square of the electric-field strength. A scan of the cou-

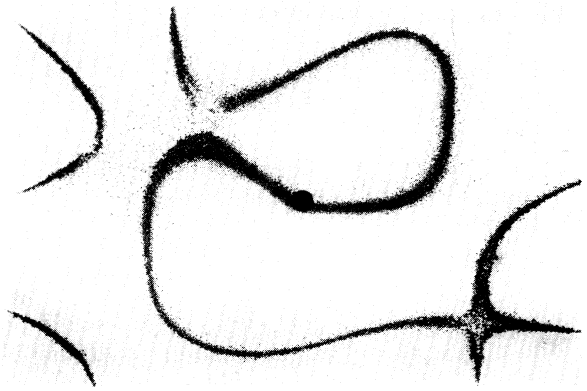

FIG. 1. Chladni figure on a glass plate of the shape of a quarted Sinai billiard ($a=21$ cm, $b=14$ cm, $r=5$ cm) is fixed in the center and excited to vibrations by a loudspeaker. The nodal lines of the vibrations are made visible by grains of semolina distributed over the plate. Typical vibration frequencies are in the range 100 to 2000 Hz.

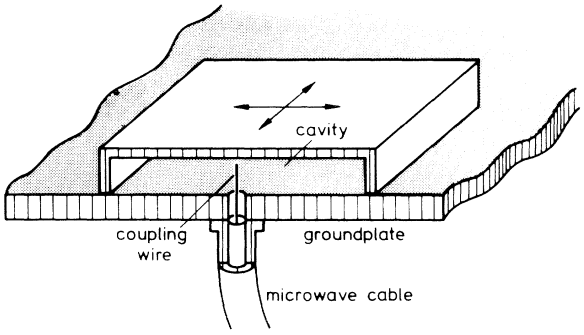

FIG. 2. Sketch of the experimental setup.

pling wire over the area thus allows the determination of E^2 as a function of the position (in the present experiment a scalar network analyzer was used, with a vector network analyzer even the determination of the sign of E would be possible). Because of the one-to-one correspondence between E^2 and the absolute square of the quantum-mechanical wave function $|\varphi|^2$ a measurement of the reflected microwave power P as a function of frequency and position of the coupling wire yields directly the quantity

$$P(q,k)\sim\sum_n \frac{\lambda}{(E-E_n)^2+\lambda^2}|\varphi(q)|^2\sim \mathrm{Im}G(q,q,E-i\lambda)\,. \tag{4}$$

In Eq. (4) E corresponds to the square of the wave number $k=2\pi\nu/c$, where ν is the microwave frequency. λ is the experimentally observed width of the resonances, limited because of the loss of microwave energy in the walls of the resonator [in reality λ differs from resonance to resonance; therefore Eq. (4) is only approximately correct].

The described procedure has one drawback. The very existence of the coupling wire modifies the spectrum of the resonator [12], and a displacement of the coupling wire leads to a shift of the resonances of up to several MHz. The maximum shift is observed at sites where the wave function takes its maximum value, whereas at the nodal lines the shift is zero. Therefore the nodal pattern is undisturbed by the measurement, whereas deviations are expected near the maxima of the wave functions.

The sketch of the experimental setup is shown in Fig. 2. The upper part of the resonator can be moved with respect to the ground plate. The coupling wire with a diameter of 0.5 mm enters through a hole in the ground plate. To improve the electrical contact between the two parts, an iron weight was placed upon the resonator. The quality figure of the resonator was about 2000, resulting in linewidths of several MHz. The microwave frequency was varied between 0.4 and 18 GHz using a Hewlett-Packard microwave generator 8350B; the reflected power was registered with a scalar network analyzer 8757A. The resonator had the shape of a quartered stadium (see Fig. 3). The position of the wire was scanned in steps of 0.5 cm in both directions yielding a total of 1555 pixels.

From the depths of the resonances the wave functions were obtained as described above. Up to now, wave functions for the first 80 eigenfrequencies were obtained. The shift of the resonances upon variation of the coupling wire complicates the reconstruction of the wave function for frequencies above 7 GHz, as here the shift comes into the order of magnitude of the distance between successive eigenvalues. As the measurements were performed in the quartered stadium only wave functions with odd-odd parity were registered. Figure 3 shows a selection of the results. The wave functions shown in Figs. 3(a)–3(c) are readily associated with periodic orbits known from literature, namely, the "bouncing ball," the double diamond, or the "whispering gallery" orbits. Some of the wave functions show distinct scars. Figure 3(d) shows a wave function belonging to one of the highest frequencies analyzed up to now. Here the disturbing influence of the coupling wire becomes manifest. While the nodal pattern is still clearly discernible, near the expected wave-function maxima one observes minima. It should be possible to reduce this effect by using coupling wires with smaller diameters. In principle diameters of the order of the skin depth (amounting to about 1 μm in the applied microwave range) should be sufficient for the irradiation of the microfrequency.

Using our experimental data we are able to check the validity of the semiclassical approximation (2) for the Green's function. Neglecting the influence of the damping, one obtains from Eqs. (2) and (4) the following expression for $P(q,k)$:

$$P(q,k)\sim \mathrm{Im}\sum_r \{i^{-3/2}|\Delta_r|^{1/2}\exp(ikl_r-i\pi n_r)\}\,, \tag{5}$$

where the sum is over all trajectories, not necessarily

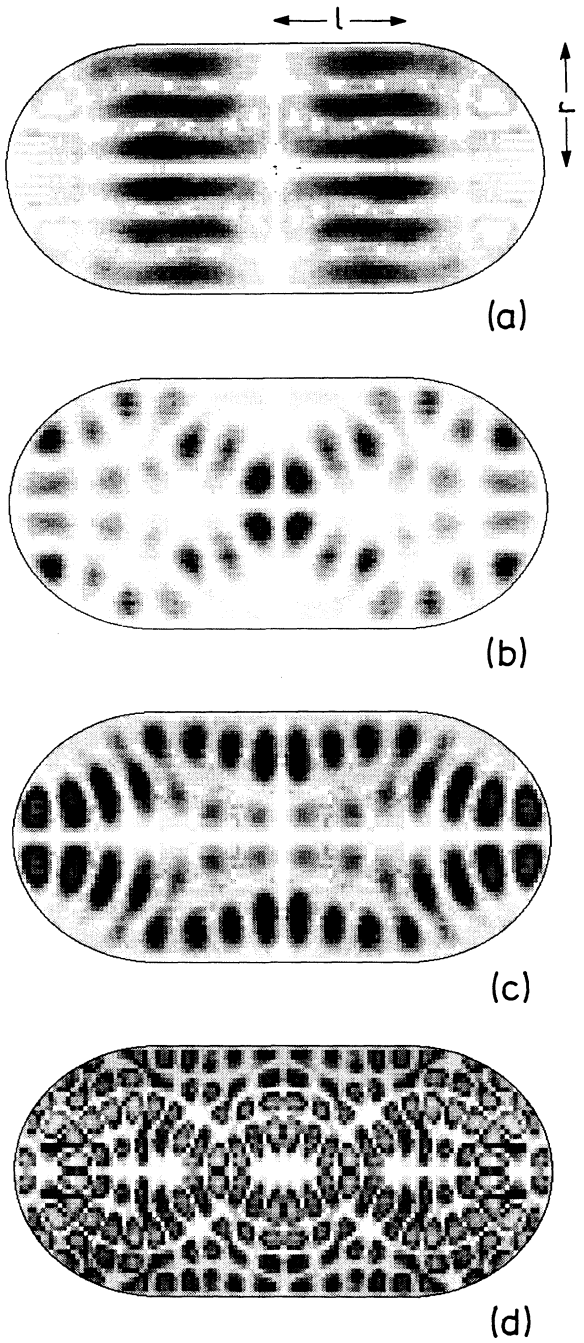

FIG. 3. Selection of stadium eigenfunctions with frequencies (a) 3.384 GHz, (b) 3.865 GHz, (c) 4.056 GHz, and (d) 7.250 GHz. The measurements were performed in a resonator of the shape of a quartered stadium ($l=18$ cm, $r=13.5$ cm). In the illustration the stadium was completed by twofold reflection. High amplitudes of the electric field are shown in black; nodal lines are white.

periodic, starting from and ending at point q. l_r is the length and n_r is the number of reflections of the respective trajectory. Therefore the Fourier transform of $P(q,k)$ with respect to k,

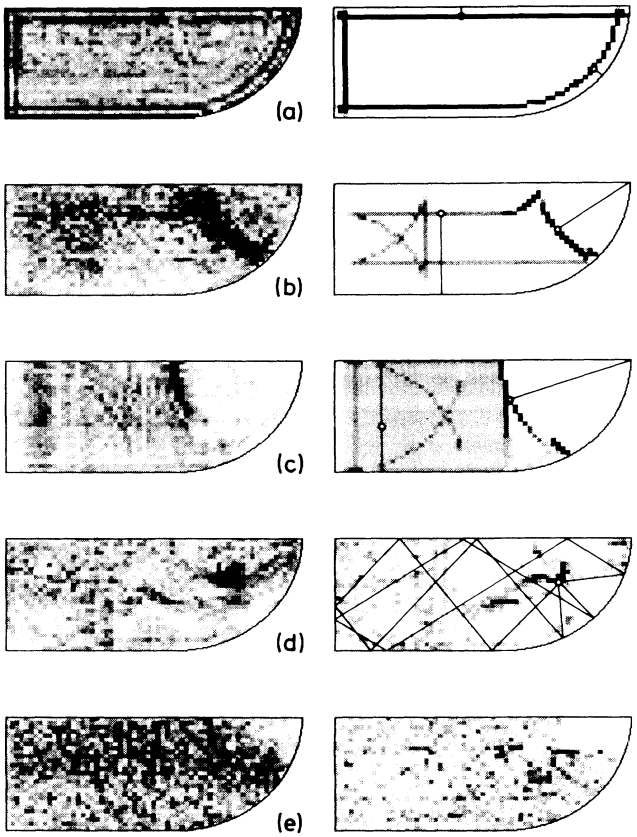

FIG. 4. Fourier transform $\hat{P}(q,l)$ of the experimentally determined eigenfunction spectrum [see Eq. (6)] as a function of position q for (a) $l=2.4$ cm, (b) 19.5 cm, (c) 27.4 cm, (d) 84.1 cm, and (e) 186.0 cm (left column). The classical counterpart calculated from closed classical trajectories [see Eq. (5)] is shown in the right column. For details see text.

$$\hat{P}(q,l)=\int P(q,k)\exp(-ikl)dk\,, \tag{6}$$

should project all contributions of paths with length l out of the sum (5). The well-known divergence problems associated with Eq. (2) [13] are no longer present in Eq. (6), as only trajectories with length l contribute to $\hat{P}(q,l)$. Its number is always finite (with the possible exception of focal points). In I an analogous procedure was applied to the eigenfrequency spectrum which is obtained by integrating expression (5) over q.

The left part of Fig. 4 shows $|\hat{P}(q,l)|$ for a number of selected l values. The Fourier transform was applied directly to the raw data, thus neglecting the influence of the coupling wire. Nevertheless, closed paths are easily recognized. For small l values the only way to get a closed path is to start at distance $l/2$ from a boundary, go directly to this boundary, and return after a reflection to the starting point [Fig. 4(a)]. For larger l values multiple reflections become possible [Fig. 4(b)]. In Fig. 4(c) the l value corresponds approximately to the length of the bouncing ball orbit. Here every point between the long

sides of the billiard is starting and end point of a closed orbit, leading to a more or less uniform coloring of this region, whereas the region within the quarter circle is colored only weakly. Similar patterns are obtained at multiples of the length of the bouncing ball orbit. At several l values foci show up [Fig. 4(d)]. Here the focusing property of the circle takes effect. At lengths above about 1.5 m the structures disappear more and more. There are, however, exceptions as shown in Fig. 4(e). Here closed trajectories exist for most points in the stadium, but apart from a small region near the upper right corner.

This discussion has already shown that the measured eigenfunctions can be interpreted qualitatively in terms of classical closed trajectories. For a quantitative comparison the right-hand side of Eq. (5) has to be calculated. Instead of calculating the $|\Delta_r|^{1/2}$, which would require one to determine the monodromy matrix for every individual trajectory [6], a brute force method was applied. First the area of the billiard was subdivided into pixels in the same way as in the measurement. Then trajectories were started in different directions in steps of 1° from the center of each pixel [in Fig. 4(e) a step width of 0.25° was chosen to improve the statistics). Whenever a trajectory reached its starting pixel after length l, a corresponding array variable was increased or decreased by 1, depending on the number of reflections. The value calculated for a pixel is proportional to the density of returning trajectories, i.e., to Δ_r [see the discussion following Eq. (3)]. This is just the square of the weight factor of the trajectory in the semiclassical Green's function. Up to this square, which was not corrected for, the described procedure is therefore able to reproduce expression (6) *quantitatively* (provided that the number of trajectories is sufficiently large). On the right-hand side of Fig. 4 the absolute values of the obtained array variables are plotted. One observes a nearly complete correspondence between the figures on the left-hand side, obtained from the wave functions, and their classical counterparts, obtained from classical trajectories. This shows that Gutzwiller's semiclassical approximation of the Green's function is able to account not only for eigenvalue spectra but also for eigenfunction patterns. In other words, geometrical optics and the de Broglie relation are sufficient to understand both billiard eigenvalue and eigenfunction properties. One point not yet mentioned remains a bit mysterious. To arrive at the correspondence displayed in Fig. 4 it was necessary to reduce the lengths belonging to the figures in the left column by 3 cm. It seems that the coupling wire leads to an effective increase of the lengths of the closed trajectories. Apart from this fact the coupling wire, though changing spectrum and eigenfunctions moderately, is not able to disturb the correspondence between eigenfunctions and classical trajectories noticeably.

This work has shown that the mapping of billiard eigenfunctions by means of a microwave analog is easily possible. It has further demonstrated that the range of applicability of the semiclassical approximation of the Green's function goes far beyond the interpretation of spectra alone. Further attractive microwave applications lie probably in the field of scattering and localization in disordered media. In a similar way as described in this work it should be possible to study enhanced backscattering, localization of wave functions, etc., within an array of random scatterers. Indeed first experiments in this direction have recently been performed though with a somewhat different technique [14].

We are grateful to B. Eckhardt for numerous fruitful discussions and for valuable suggestions to the manuscript. K.-H. Kretschmer assisted in producing the Chladni figures. The work was sponsored by the Deutsche Forschungsgemeinschaft via the Sonderforschungsbereich "Nichtlineare Dynamik."

Note added.— After the completion of this work we became aware of a recent publication on the same topic [15]. In contrast to the present work the author did not use the reflected microwave power but the shift of the eigenfrequencies to map the eigenfunctions.

[1] M. C. Gutzwiller, *Chaos in Classical and Quantum Mechanics* (Springer, New York, 1990).
[2] S. W. McDonald and A. N. Kaufman, Phys. Rev. Lett. **42**, 1189 (1979).
[3] S. W. McDonald and A. N. Kaufman, Phys. Rev. A **37**, 3067 (1988).
[4] E. J. Heller, Phys. Rev. Lett. **53**, 1515 (1984).
[5] E. J. Heller, P. W. O'Connor, and J. Gehlen, Phys. Scr. **40**, 354 (1989).
[6] E. B. Bogomolny, Physica (Amsterdam) **31D**, 169 (1988).
[7] M. C. Gutzwiller, J. Math. Phys. **12**, 343 (1971).
[8] M. V. Berry and M. E. Mount, Rep. Prog. Phys. **35**, 315 (1972).
[9] H.-J. Stöckmann and J. Stein, Phys. Rev. Lett. **64**, 2215 (1990).
[10] F. Melde, *Akustik* (Brockhaus, Leipzig, 1883), p. 191.
[11] R. Blümel *et al.*, Phys. Rev. A **45**, 2641 (1992).
[12] F. Haake, G. Lenz, P. Šeba, J. Stein, H.-J. Stöckmann, and K. Życzkowski, Phys. Rev. A **44**, 6161 (1991).
[13] B. Eckhardt and E. Aurell, Europhys. Lett. **9**, 509 (1989).
[14] S. L. McCall, P. M. Platzman, R. Dalichaouch, D. R. Smith, and S. Schultz, Phys. Rev. Lett. **67**, 2017 (1991).
[15] S. Sridhar, Phys. Rev. Lett. **67**, 785 (1991).

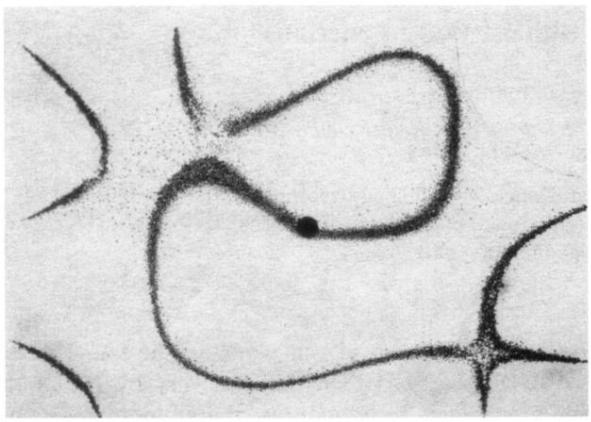

FIG. 1. Chladni figure on a glass plate of the shape of a quarted Sinai billiard ($a=21$ cm, $b=14$ cm, $r=5$ cm) is fixed in the center and excited to vibrations by a loudspeaker. The nodal lines of the vibrations are made visible by grains of semolina distributed over the plate. Typical vibration frequencies are in the range 100 to 2000 Hz.

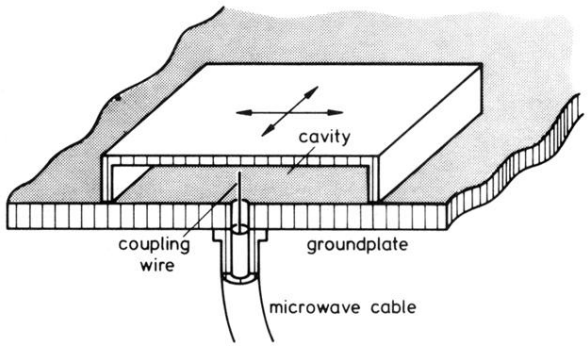

FIG. 2. Sketch of the experimental setup.

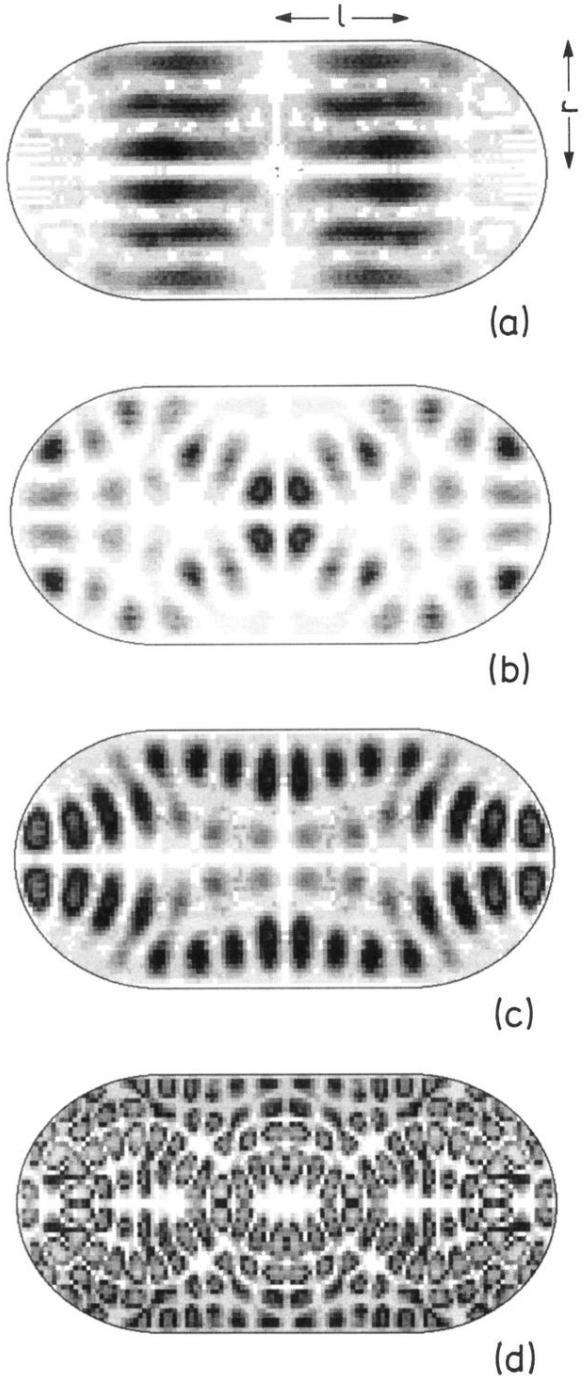

FIG. 3. Selection of stadium eigenfunctions with frequencies (a) 3.384 GHz, (b) 3.865 GHz, (c) 4.056 GHz, and (d) 7.250 GHz. The measurements were performed in a resonator of the shape of a quartered stadium ($l=18$ cm, $r=13.5$ cm). In the illustration the stadium was completed by twofold reflection. High amplitudes of the electric field are shown in black; nodal lines are white.

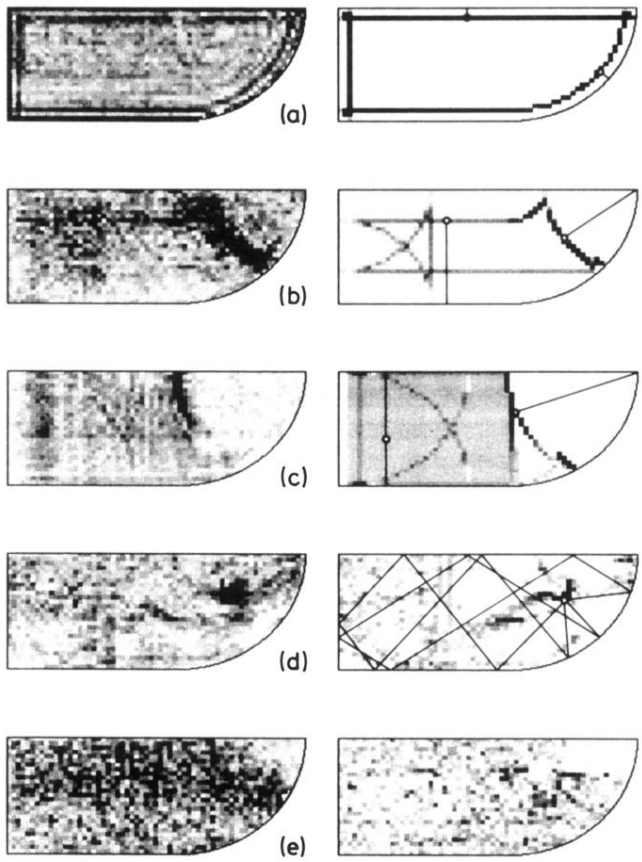

FIG. 4. Fourier transform $\hat{P}(q,l)$ of the experimentally determined eigenfunction spectrum [see Eq. (6)] as a function of position q for (a) $l=2.4$ cm, (b) 19.5 cm, (c) 27.4 cm, (d) 84.1 cm, and (e) 186.0 cm (left column). The classical counterpart calculated from closed classical trajectories [see Eq. (5)] is shown in the right column. For details see text.